Dynamics of $F = 2$ Spinor Bose-Einstein Condensates

H. Schmaljohann,[1] M. Erhard,[1] J. Kronjäger,[1] M. Kottke,[2] S. van Staa,[1] L. Cacciapuoti,[2] J. J. Arlt,[2] K. Bongs,[1] and K. Sengstock[1]

[1]*Institut für Laser-Physik, Universität Hamburg, Luruper Chaussee 149, 22761 Hamburg, Germany*
[2]*Institut für Quantenoptik, Universität Hannover, Welfengarten 1, 30167 Hannover, Germany*

(Received 14 August 2003; published 28 January 2004)

We experimentally investigate and analyze the rich dynamics in $F = 2$ spinor Bose-Einstein condensates of ^{87}Rb. An interplay between mean-field driven spin dynamics and hyperfine-changing losses in addition to interactions with the thermal component is observed. In particular, we measure conversion rates in the range of 10^{-12} cm^3 s^{-1} for spin-changing collisions within the $F = 2$ manifold and spin-dependent loss rates in the range of 10^{-13} cm^3 s^{-1} for hyperfine-changing collisions. We observe polar behavior in the $F = 2$ ground state of ^{87}Rb, while we find the $F = 1$ ground state to be ferromagnetic. We further see a magnetization for condensates prepared with nonzero total spin.

DOI: 10.1103/PhysRevLett.92.040402 PACS numbers: 03.75.Mn, 03.75.Hh, 34.50.Pi

The investigation of atomic spin systems is central for the understanding of magnetism and a highly active area of research, e.g., with respect to magnetic nanosystems, spintronics, and magnetic interactions in high T_c superconductors. In addition, entangled spin systems in atomic quantum gases show intriguing prospects for quantum optics and quantum computation [1–5]. Bose-Einstein condensates (BEC) of ultracold atoms offer new regimes for studies of collective spin phenomena [6–13]. BECs with a spin degree of freedom are special in the sense that their order parameter is a vector in contrast to the "common" BEC where it is a scalar. Recent extensive studies have been made in optically trapped ^{23}Na in the $F = 1$ state [10–13]. In addition, evidence of spin dynamics was demonstrated in optically trapped ^{87}Rb in the $F = 1$ state [14]. There is current interest in extending the systems under investigation to $F = 2$ spinor condensates [15–20], which add significant new physics. $F = 2$ spinor condensates offer richer dynamics and an additional magnetic phase, the so-called cyclic phase [16,18].

In this Letter, we present first studies of optically trapped ^{87}Rb spinor condensates in the $F = 1$ and $F = 2$ hyperfine states. We measure rates for spin-changing collisions for different channels within the $F = 2$ manifold and discuss the steady state for various initial conditions. Additionally, we observe and discuss the thermalization of dynamically populated m_F condensates. We also present measurements of spin-dependent hyperfine decay rates of the $F = 2$ state in ^{87}Rb, as a key to further understanding the intensively studied collisional properties of ^{87}Rb [21,22].

Our experimental setup consists of a compact double MOT apparatus which produces magnetically trapped ^{87}Rb Bose-Einstein condensates in the $F = 2, m_F = 2$ state. To confine the atoms independently of their spin state, they are subsequently transferred into a far detuned optical dipole trap operated at 1064 nm with trapping frequencies of $2\pi \times 891$ Hz vertically, $2\pi \times 155$ Hz horizontally, and $2\pi \times 21.1$ Hz along the beam direction. We end up with approximately 10^5 optically trapped atoms and a condensate fraction well above 60%. We are able to prepare arbitrary spin compositions using rapid adiabatic passage and controlled Landau-Zener crossing techniques [23] at an offset field around 25 G. After initial state preparation, the magnetic field is lowered to a value of typically 340($\pm$20) mG, with a field gradient below 15 mG/cm [24], to ensure a well-defined quantization axis and a good overlap of the different m_F states during spin dynamics [25,26]. Stored in the optical trap, the condensate spin degree of freedom can now evolve under well-controlled conditions during a variable hold time. Because of interatomic interactions, initially prepared m_F components can evolve into other m_F components, e.g., by processes such as $|0\rangle + |0\rangle \leftrightarrow |+1\rangle + |-1\rangle$, while—disregarding atomic losses—the total spin is conserved. This process is expected to end in the spinor ground state distribution showing the hyperfine dependent magnetic properties of the atomic species under investigation. Experimentally, we detect different spin components by spatially separating them with a Stern-Gerlach method during time of flight (after switching off the trapping potential). Absorption imaging is then used to evaluate the respective spatial density distributions as well as the number of atoms and thermal fractions for each spin component. Figure 1 shows typical spinor condensate evolutions for different starting conditions. These pictures demonstrate a rich spectrum of spin dynamics in $F = 2$ systems, caused by an intriguing interplay of spin component coupling and spin-dependent losses. In the following, we will investigate these processes separately.

We analyze the observed spinor evolution in a mean-field approach [16,18,27,28], in which the properties of a spinor condensate are determined by a spin-dependent energy functional. Extending the approach of [18] by the experimentally relevant quadratic Zeeman

 © 2004 The American Physical Society

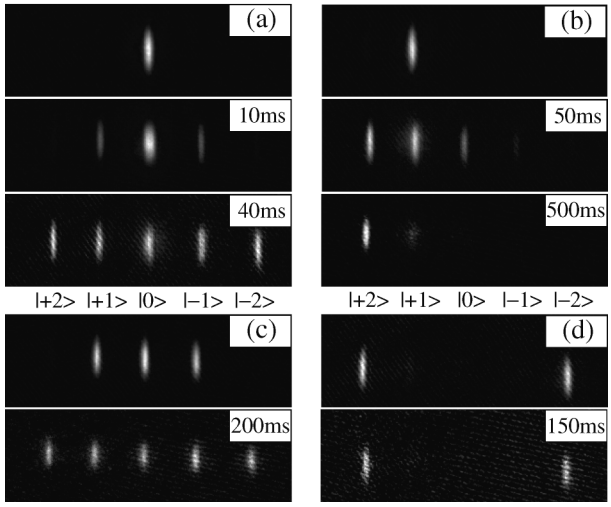

FIG. 1. Time-dependent observation of different m_F components starting from the initially prepared states denoted by (a)–(d). Shown are spinor condensates separated by a Stern-Gerlach method (time of flight 31 ms).

energy term, we determine the following functional for $F = 2$ systems:

$$K_{\text{spin}} = c_1\langle \boldsymbol{F}\rangle^2 + \tfrac{4}{5}c_2|\langle s_-\rangle|^2 - p\langle F_z\rangle - q\langle F_z^2\rangle, \quad (1)$$

where $\langle \boldsymbol{F}\rangle$, $\langle F_z\rangle$, and $\langle s_-\rangle$ denote the expectation values of the spin vector, its z component, and the spin-singlet pair amplitude. The experimentally controllable parameters p and q span the phase space for the system. p represents the mean spin of the system while q is the quadratic Zeeman energy, representing the magnetic offset field.

The spin-dependent mean field is characterized by the parameters $c_1 = [(4\pi\hbar^2 n)/m][(a_4 - a_2)/7]$ and $c_2 = [(4\pi\hbar^2 n)/m][(7a_0 - 10a_2 + 3a_4)/7]$, introducing the s-wave scattering length a_f for collisions involving a total spin f of the colliding pair. In the following, the $F = 2, m_F = X$ state is denoted by $|X\rangle$. For simplicity, relative phases in mixtures are neglected. The c_1 term includes all couplings of states with $\Delta m_F = \pm 1$, e.g., $|0\rangle + |0\rangle \leftrightarrow |+1\rangle + |-1\rangle$. The c_2 term includes the only possible coupling with $\Delta m_F = \pm 2$: $|0\rangle + |0\rangle \leftrightarrow |+2\rangle + |-2\rangle$. The magnitude of these terms is connected to the time scales of spin dynamics, and their relative strengths indicate the initially dominant channels. For the calculated scattering lengths and our initial experimental conditions (mean density $n \approx 4 \times 10^{14}$ cm^{-3}), the energy ranges for the different terms are spin-independent mean field $k_B \times$ 150 nK, spin-dependent mean field $c_1{:}k_B \times$ 0–10 nK, $c_2{:}k_B \times$ 0–0.2 nK, and quadratic Zeeman energy $q{:}k_B \times$ 0–1.6 nK. Because of conservation of total spin, the linear Zeeman energy does not affect the system.

Minimizing the energy functional, Eq. (1) leads to the parameter-dependent ground state spin composition of the system, reflecting its magnetic properties [26]. Theory predicts ^{87}Rb in $F = 2$ to be polar ($c_1 - c_2/20 > 0$ and $c_2 < 0$), but close to the border to the so-called cyclic phase ($c_1 > 0$ and $c_2 > 0$) as opposed to the ferromagnetic phase ($c_1 < 0$ and $c_1 - c_2/20 < 0$) [16,19]. In the absence of magnetic fields, the polar state is given by any rotation of the $|0\rangle$ state, the ground state of the ferromagnetic phase is any rotation of the $|+2\rangle$ state, and the cyclic phase is described by a superposition of the states $|+2\rangle$, $|0\rangle$, and $|-2\rangle$.

Experimentally, we find the system dominated by three processes, setting different time scales, in increasing order: spin dynamics, two-body hyperfine losses, and three-body recombination. This hierarchy allows us to separately analyze individual interaction processes, which are exemplarily given in Fig. 2.

In a first set of measurements, we study the evolution of spinor condensates starting from different spin states. Figure 2(a) shows the evolution of the relative occupation of the different m_F components of a $F = 2$ spinor condensate initially prepared in the state $|0\rangle$, also shown in Fig. 1(a). This example clearly demonstrates that spin evolution takes place predominantly between neighboring spin states, as expected from coupling via the dominating c_1 term discussed above. Thus, first the components $|\pm 1\rangle$ and only afterwards the $|\pm 2\rangle$ states are populated. Interestingly, there is a delay in the occupation of $|\pm 1\rangle$ and a further delay in the occupation of $|\pm 2\rangle$ states. The latter can be intuitively explained since there must first be some occupation in the $|\pm 1\rangle$ states before the fully stretched states can be occupied. The origin of the initial delay as well as the "overshoot" of the $|\pm 1\rangle$ occupation is still under investigation. As an interesting feature, Fig. 2(a) shows evidence of spinor oscillations on a 100 ms time scale around equipartition. This indicates a coherent evolution between the different m_F components, with only

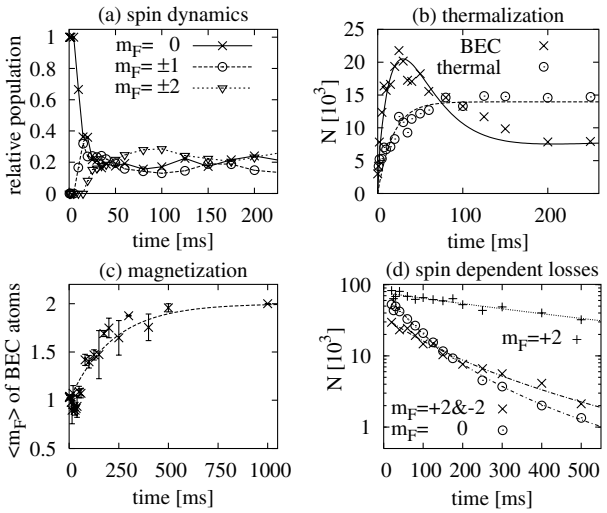

FIG. 2. Spin dynamics and spin-dependent losses. (a) Relative population of the m_F states of a condensate initially prepared in $|0\rangle$. (b) Thermalization of a BEC in the $|+2\rangle$ state from initially $|0\rangle + |+1\rangle$. (c) Total spin of the condensate initially prepared in $|+1\rangle$. (d) Decay curves for total number of condensed atoms in all m_F states, given for different initial m_F preparations.

minor influence of the thermal cloud on this time scale (see also [29]).

We always observe that spin dynamics is significantly quicker than thermalization in the $F = 2$ state. Spin dynamics leads to the formation of pure condensate wave functions in new spin states, which subsequently thermalize on a much longer time scale. This opens a new way to study thermalization effects with an independently tunable heat bath. In Fig. 2(b), the condensate and thermal fractions of the newly created $|+2\rangle$ state, starting with a mixture of the states $|+1\rangle$ and $|0\rangle$, are plotted. At first the condensate in the $|+2\rangle$ state is almost pure. This can be intuitively understood, as spin dynamics predominantly occurs in the high density condensate fraction on a time scale of the order of 10 ms. The subsequent buildup of a thermal cloud in the newly populated spin states takes place within a significantly longer time, of the order of 50 ms. Dominant effects contributing to the thermalization of the new spin state are the interaction of the new spin condensate with the parent thermal cloud (''melting''), and spin dynamics of the parent condensate fraction with its thermal cloud leading to an occupation of the new component thermal cloud. In this respect, spinor condensates are a possible new tool for investigation of finite temperature effects (see also [30]).

In order to draw a more complete picture of spin dynamics in $F = 2$ systems, we now investigate the evolution of a variety of initial states as summarized in Table I. In this table, we give estimates for the initial spin dynamics rates for different channels as well as the experimentally observed ''final'' distribution. The rates are intended for comparison with loss rates and between the different spin channel rates. They were obtained using the total ensemble density, number of BEC atoms in the prepared m_F components, and the initial slope of a phenomenological exponential fit to the respective spin component population curves: $G_{\to|X\rangle} = [(dN_{|X\rangle})/(dt)] \times (N_{\text{initial}}\langle n_{\text{initial}}\rangle)^{-1}$. Note that for elastic collisions $G_{\text{el}} \approx 10^{-11}$ cm^3 s^{-1}. Looking at the spin-changing processes, we find the rate for $|0\rangle \to |\pm 1\rangle$ at short time scales similar to the rate $|\pm 1\rangle \to |0\rangle$ as one would expect for a reversible or coherent process. In contrast, at longer time scales, the system evolves as expected into a time-independent distribution of m_F states. As a main result, our measurements show the stability of a mixture of $|\pm 2\rangle$ [see Table I and Fig. 1(d)], for which we find no spatial separation of the two components in the trap. This is clear evidence of *polar* behavior for $F = 2$ spinor condensates of ^{87}Rb.

TABLE I. Spin evolution for different preparations.

Initially prepared m_F states	Initial total spin	Initial channels into m_F state G [10^{-13} cm^3 s^{-1}]	Finally populated m_F states
$\|0\rangle$	0	$\to \|\pm 1\rangle \approx 21.0$	Equipartition
$\|+1\rangle + \|-1\rangle$	0	$\to \|0\rangle \approx 26.9$ $\to \|\pm 2\rangle \approx 4.6$	Equipartition
$\|+1\rangle + \|0\rangle + \|-1\rangle$	0	$\to \|\pm 2\rangle \approx 5.0$	Equipartition
$\|+2\rangle + \|-2\rangle$	0	$\cdots$	$\|+2\rangle + \|-2\rangle$
$\|+2\rangle + \|0\rangle + \|-2\rangle$	0	$\to \|\pm 1\rangle < 0.1$	$\|+2\rangle + \|-2\rangle$
$\|+2\rangle + \|-1\rangle$	1/2	$\cdots$	$\|+2\rangle$
$\|+1\rangle + \|0\rangle$	1/2	$\to \|+2\rangle \approx 21.7$ $\to \|-1\rangle \approx 19.2$	$\|+2\rangle$
$\|+1\rangle$	1	$\to \|+2\rangle \approx 22.4$ $\to \|0\rangle \approx 12.2$ $(\to \|-1\rangle \approx 4.7)$	$\|+2\rangle$
$\|+2\rangle$	2	$\cdots$	$\|+2\rangle$

Some initial preparations with zero total spin end up with all m_F components equally populated [see also Figs. 1(a) and 1(c)]. For our experimental parameters, a mixture of all m_F components is not a ground state for any phase in the mean-field description, due to the quadratic Zeeman energy. The observed behavior might be due to a lack of time to reach the ground state, as spin-dependent losses depopulate the condensate before thermal equilibrium is reached.

Remarkably, if the atoms are prepared in superpositions which are ground states for the *cyclic phase*, we observe very slow dynamics. First the mixture of $|+2\rangle + |0\rangle + |-2\rangle$, which is the ground state of the cyclic phase with total spin zero [20] shows nearly no spin dynamics. If starting with $|+2\rangle + |-1\rangle$ as a ground state for the cyclic phase at $B > 0$ [26] with nonzero spin, we do not observe any spin dynamics. These cases are particularly surprising, as the states $|0\rangle$ alone as well as $|+1\rangle$ alone show fast spin dynamics as can be seen in Figs. 1(a) and 1(b). In the mixtures, however, we observe only a faster decay of the $|0\rangle$ and $|-1\rangle$ component compared to $|\pm 2\rangle$. Concluding this, the stability of the $|\pm 2\rangle$ mixture demonstrates polar behavior of $F = 2$ ^{87}Rb atoms, and in addition the slow dynamics of prepared cyclic ground states shows the $F = 2$ state to be close to the cyclic phase [31].

An important point in the dynamics of spinor condensates is total spin conservation. This is directly observed in the rates for all spin preparations (see rates Table I). Note that this is also true for the case starting with $|+1\rangle$ due to a fast production of the $|-1\rangle$ component.

Investigating spinor condensates with initial spin $\neq 0$, one finds that the combination of spin dynamics and spin-dependent hyperfine losses (see below) leads to a loss induced magnetization during the evolution to the final state, e.g., if starting in the $|+1\rangle$ state [Figs. 1(b) and 2(c)]. As seen in the figure, spin dynamics first spreads the population over different m_F states, which then decay into the lower hyperfine state. The remaining condensate always ends up in the fully stretched state due to the fact that only the fully stretched component is immune to hyperfine-changing collisions. The magnetization process is inhibited only for a symmetric initial state having total spin zero.

Next, we focus on hyperfine-changing collisions (i.e., involving transitions $F = 2 \to F = 1$) as a special case of spin relaxation dynamics. The release of hyperfine

energy in these collisions leads to immediate loss of the collision partners from the trap. This loss process usually takes place on very short time scales, prohibiting the observation of spin dynamics in the upper hyperfine level, e.g., of ^{23}Na [15]. The relatively low hyperfine loss rates we find for ^{87}Rb are due to a coincidental destructive interference of decay paths [6,32]. Figure 2(d) shows the decay of Bose-Einstein condensates of ^{87}Rb prepared in different m_F states/mixtures. The decay of the stretched state $|+2\rangle$ is dominated by three-body recombination and was measured by [33] to be $L = 1.8 \times 10^{-29}$ cm^6 s^{-1}, a value which also fits our data. The equal superposition of the $|+2\rangle$ and $|-2\rangle$ states is special in the sense that we observe no spin dynamics in this case. The hyperfine-changing collisions can thus occur only via collisions of the type $|2, +2\rangle + |2, -2\rangle \rightarrow |1, m_1\rangle + |F, m_2\rangle (F = 1, 2)$. We deduce the two-body rate $G = 6.6(\pm 0.9) \times 10^{-14}$ cm^3 s^{-1}, which leads to a much faster decay than three-body losses for the pure $|+2\rangle$ state [Fig. 2(d)]. The dependence of the hyperfine-changing collision rate on the number of decay channels involved becomes obvious observing the decay of a condensate initially prepared in the state $|0\rangle$ [see Fig. 2(d)]. It is important to note that in this case spin dynamics more rapidly ($\leq$25 ms) distributes the population almost equally over all m_F states. The decay curve (of initially $|0\rangle$) thus effectively represents the loss of a spin state equipartition, which has access to all possible channels. We determine the mean two-body decay rate for this case to be $G = 10.2(\pm 1.3) \times 10^{-14}$ cm^3 s^{-1}.

Finally, we have also studied spinor condensates in the $F = 1$ state where we observe slow spin dynamics on a time scale of seconds such as in the case of ^{23}Na in $F = 1$ [10]. Comparing the $F = 1$ with the $F = 2$ case in the spin-dependent energy functional (1), the sign of q changes and there is no c_2 term. Starting in the superposition state $|1, \pm 1\rangle$, we observe the creation of the $|1, 0\rangle$ component. The final state with all m_F components populated and spatially mixed is reached after about 7 s. According to the phase diagrams of [10], we have thus shown that ^{87}Rb *in the* $F = 1$ *state is ferromagnetic* ($a_0 > a_2$) as predicted by [19,27].

In conclusion, we have presented studies of various aspects of $F = 2$ spinor condensates in ^{87}Rb. In particular, we have discussed rates for spin dynamics as well as the evolution into the magnetic ground state. Furthermore, we have investigated spin-dependent hyperfine-changing collisions and thermalization effects in newly created spin components during spinor evolution. These studies have demonstrated the feasibility of ^{87}Rb condensates as a model for $F = 2$ spin systems, added data to the collisional properties of ^{87}Rb, and opened a new path for finite temperature studies. As a key result, we measure ^{87}Rb in the $F = 1$ state to be ferromagnetic and observe polar behavior for the $F = 2$ state.

We acknowledge stimulating contributions by W. Ertmer and support from the *Deutsche Forschungsgemeinschaft* in the SFB 407 and the SPP 1116.

Note added.—After submission of this Letter, related work of Chang *et al.* appeared [34].

[1] H. Pu and P. Meystre, Phys. Rev. Lett. **85**, 3987 (2000).
[2] L. You and M. S. Chapman, Phys. Rev. A **62**, 052302 (2000).
[3] A. Sørensen, L.-M. Duan, J. Cirac, and P. Zoller, Nature (London) **409**, 63 (2001).
[4] B. Julsgaard, A. Kozhekin, and E. Polzik, Nature (London) **413**, 400 (2001).
[5] O. Mandel *et al.*, Phys. Rev. Lett. **91**, 010407 (2003).
[6] C. J. Myatt *et al.*, Phys. Rev. Lett. **78**, 586 (1997).
[7] D. S. Hall *et al.*, Phys. Rev. Lett. **81**, 1539 (1998).
[8] M. R. Matthews *et al.*, Phys. Rev. Lett. **81**, 243 (1998).
[9] J. M. McGuirk *et al.*, Phys. Rev. Lett. **89**, 090402 (2002).
[10] J. Stenger *et al.*, Nature (London) **396**, 345 (1999).
[11] H.-J. Miesner *et al.*, Phys. Rev. Lett. **82**, 2228 (1999).
[12] D. M. Stamper-Kurn *et al.*, Phys. Rev. Lett. **83**, 661 (1999).
[13] A. E. Leanhardt *et al.*, Phys. Rev. Lett. **90**, 140403 (2003).
[14] M. Barrett, J. Sauer, and M. S. Chapman, Phys. Rev. Lett. **87**, 010404 (2001).
[15] A. Görlitz *et al.*, Phys. Rev. Lett. **90**, 090401 (2003).
[16] C. V. Ciobanu, S.-K. Yip, and T.-L. Ho, Phys. Rev. A **61**, 033607 (2000).
[17] T.-L. Ho and L. Yin, Phys. Rev. Lett. **84**, 2302 (2000).
[18] M. Koashi and M. Ueda, Phys. Rev. Lett. **84**, 1066 (2000).
[19] N. N. Klausen, J. L. Bohn, and C. H. Greene, Phys. Rev. A **64**, 053602 (2001).
[20] M. Ueda and M. Koashi, Phys. Rev. A **65**, 063602 (2002).
[21] E. G. M. van Kempen, S. J. J. M. F. Kokkelmans, D. J. Heinzen, and B. J. Verhaar, Phys. Rev. Lett. **88**, 093201 (2002).
[22] A. Marte *et al.*, Phys. Rev. Lett. **89**, 283202 (2002).
[23] M.-O. Mewes *et al.*, Phys. Rev. Lett. **78**, 582 (1997).
[24] The calibration of the offset field is done by Landau-Zener transitions at different field values. The field gradient is deduced from time-of-flight trajectories of condensates in the $m_F = +2$ and $m_F = -2$ states.
[25] The desired initial state is preserved up to this time as spin dynamics at high magnetic field values is suppressed.
[26] Calculations on spinor properties including the quadratic Zeeman energy will be presented elsewhere.
[27] T.-L. Ho, Phys. Rev. Lett. **81**, 742 (1998).
[28] T. Ohmi and K. Machida, J. Phys. Soc. Jpn. **67**, 1822 (1998).
[29] J. M. McGuirk, D. M. Harber, H. J. Lewandowski, and E. A. Cornell, Phys. Rev. Lett. **91**, 150402 (2003).
[30] H. J. Lewandowski, J. M. McGuirk, D. M. Harber, and E. A. Cornell, Phys. Rev. Lett. **91**, 240404 (2003).
[31] There might be the option, that ^{87}Rb ($F = 2$) is cyclic at $B = 0$, but shifted into the polar phase by our offset field.
[32] P. S. Julienne, F. H. Mies, E. Tiesinga, and C. J. Williams, Phys. Rev. Lett. **78**, 1880 (1997).
[33] J. Söding *et al.*, Appl. Phys. B **69**, 257 (1999).
[34] M.-S. Chang *et al.*, cond-mat/0309164.